JOURNAL OF MATERIALS SCIENCE 10 (1975) 1571–1581

Low-cycle fatigue-crack initiation study in René 95

M. N. MENON, W. H. REIMANN
Air Force Materials Laboratory, Wright-Patterson Air Force Base, Dayton, Ohio, USA

A microstructural study of fatigue deformation and cracking was conducted on René 95, which is a thermomechanically processed superalloy developed for use as discs in advanced gas turbine engines. Optical, replica, scanning and transmission electron microscopy were used in order to study the deformation structures and mode of cracking during crack initiation under low-cycle fatigue. As in a previous tensile study, it was found that the deformation occurred very homogeneously throughout the material. This is believed to be due to the slip dispersive effect of the substructure in the warm worked grains and the very small size of the necklace grains. The study also showed that the number of load cycles to produce crack initiation can be strongly affected by brittle constituents of the microstructure, such as MC carbides. It was found that the specimens that had shorter lives were characterized by MC carbide cracking at the site of the crack initiation, whereas those which had longer lives under the same conditions of loading and temperature were characterized by only slip band cracking with no evidence of MC carbide cracking or decohesion in influencing the initiation.

1. Introduction

Design practices for low-cycle fatigue (LCF) limited components, such as discs in advanced gas turbine engines, have been based essentially on material S/N curves generated from specimen testing. These curves give the relationship between the applied stress (or strain) per cycle and the number of cycles required to fail the specimen. For design purposes these material S/N curves are generally adjusted by some means to allow for materials variation and to ensure conservatism in the design. For a finite life component the resulting design curves define the maximum allowable stress (or strain) per flight cycle and this, in turn, is used to size the component.

Although these procedures have proven to be satisfactory from a safety and reliability standpoint, the system leaves a great deal to be desired from a cost effectiveness standpoint. Because of the conservatism of the approach, the vast majority of discs may reach the established low-cycle fatigue limit with some potentially useful life remaining. The high cost of replacement of advanced alloy discs makes it highly desirable that techniques be devised that will permit maximum utilization of these discs without any compromise of safety or reliability.

The excessive conservatism of the current design approach arises essentially because of the inherent scatter in the number of cycles required to initiate and propagate a fatigue crack to failure. Establishment of such scatter would not only provide a firmer basis for the future development of life prediction techniques, but also would give greater insight into the design of an alloy for those specific uses. It has been widely recognized that microstructure plays an important part in determining the time to initiate and to propagate a fatigue crack. While much work has been done on fatigue crack propagation of engineering size cracks, studies of initiation and early growth have not received as much attention. This study was undertaken in order to understand more fully the modes of cracking in the initial stages of low-cycle fatigue in René 95, which is an advanced superalloy used for compressor and turbine disc applications.

Prior work on wrought Udimet 700 [1] has shown that the primary mode of crack initiation in LCF in this material at room temperature was by slip band and twin boundary cracking. Subsequent work on single crystal and columnar grained Mar-M 200 [2] has revealed large pre-

cracked MC carbides (size ~ 0.09 to 0.06 mm) and to a lesser extent micropores as crack initiation points at room temperature. As the temperature was increased, indications of surface intergranular crack initiation was found in wrought Udimet 700 [3]. At 1033 K, all the crack initiation in this material was at the surface and intergranular in nature. Often, these intergranular surface cracks propagated only one grain diameter before a transition to transgranular cracking occurred. In the case of columnar and single crystal Mar-M 200, cracks still originated at the carbides and micropores at 1033 and 1200 K. However, the fracture mode became more non-crystallographic at 1200 K as compared to that at 1033 K, cracking at the latter temperature being in the Stage I mode alone [4]. On the other hand, in conventionally-cast Mar-M 200, grain boundaries were the preferred sites for crack initiation and propagation at 1033 and 1200 K. As the mode of propagation in the columnar and single crystal materials was transgranular and much slower, fatigue lives were one or two orders of magnitude higher than those of conventionally cast Mar-M 200.

In cast Udimet 500, crack initiation in LCF at 922 K occurs preferentially at surface carbide particles which cracked during testing [5]. Subsequent propagation was found to be in stage I mode at this temperature. At 1088.7 K, crack initiation occurred preferentially at grain boundaries and interdendritic carbide particles, with subsequent propagation by stage II mode.

The present investigation was undertaken to study the relationship between the low-cycle fatigue behaviour and the microstructure of René 95, which is an advanced superalloy developed by the General Electric Co. In addition to the normal precipitation and solid solution strengthening, René 95 derives part of its strength also from a residual defect structure introduced into it through thermomechanical processing (TMP). Table I gives the composition of René 95.

TABLE I Composition of René 95

C	Cr	Co	Fe	Mo	W	Ti	Al
0.16	13.8	8.1	0.18	3.55	3.53	2.46	3.41
Nb	B	Zr	Mn	Si	S	P	Ni
3.56	0.012	0.04	0.10	0.10	0.0003	0.01	Balance

2. Processing and heat-treatment

The processing starts with vacuum induction melted and vacuum arc remelted ingot, approximately 0.228 m diameter, which is given a homogenization anneal in the range 1436 to 1463 K for 3 h and then furnace cooled. The ingot is subsequently reheated to 1366 to 1410 K and the primary processing reduction is applied to bring the thickness to 40 to 50% above the final value. This is followed by a recrystallization anneal at 1436 ± 13.9 K for 1 h, which results in a uniform grain size of ASTM 3-5. The forging is cooled from the recrystallization temperature at a rate greater than 83.3 K h^{-1} to 1172 K and then air-cooled or taken to final processing. The forging is reheated to 1352 to 1380 K and the final reduction is applied resulting in a 40% to 50% decrease in thickness. This imparts residual warm work into the material and allows the grain-boundary regions to recrystallize into a necklace of very small grains.

Heat-treatment after forging consists of a 1366 K partial solutioning treatment, salt or oil quench to ⩽ 755 K and a 1033 K, 16 h ageing.

3. Experimental procedure

Fatigue testing was carried out on "hour glass" specimens, machined out of René 95 forgings. Fig. 1 gives the dimensions of the specimen. The hour glass section of the specimens were polished by hand with 6 and 1 μm diamond polishing paste using a micro-cloth. This polishing was found to be better than electrochemical polishing as the latter tended to pit the surface. The few scratches that remained after the polishing were in the longitudinal direction only. The gauge section was then etched with Walker's etch [6] for about 1 min and then a replica was taken of the etched surface.

The specimens were fatigued at 5 Hz with a maximum stress of 1275.5 MN m^{-2} and R value equal to 0.05 in a MTS hydraulic testing machine. The testing was interrupted periodically in order to replicate the development of microcracks, their linkage and propagation on the surface. These replicas were subsequently mounted on the microscope slides and observed under a Zeiss Metallograph. Selected replicas were shadowed with platinum–carbon mixture, and carbon support replica films were prepared from these for observation in an electron microscope. The fracture surfaces were examined in a scanning electron microscope (SEM).

Whenever possible, very thin sections were cut near the crack initiation and propagation regions,

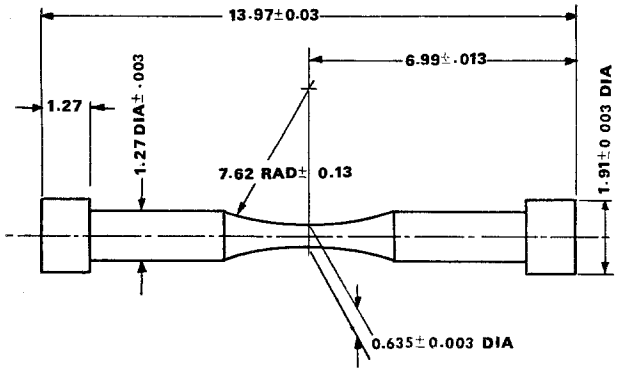

Figure 1 Dimensions of the LCF specimen (cm).

both parallel and perpendicular to the fracture surface by means of EDM and subsequently thinned in a twin-jet electropolisher for observation in the transmission electron microscope. One subscale cylindrical specimen which had a diameter of 0.41×10^{-2} m and a gauge length of 1.65×10^{-2} m was also cycled at room temperature under the same loading conditions to 8000 cycles. Thin slices from this specimen were examined for observation in the TEM.

4. Experimental results

4.1. Microstructure of necklace René 95

Fig. 2a shows the typical necklace structure of René 95 in which warm-worked grains having an average size of 75 μm are surrounded by a necklace of very small recrystallized grains (size 4 μm). The warm-worked grains have a uniform distribution of intermediate-sized γ' precipitates (size 0.5 μm) which give a darker shade to these grains in the optical micrograph. The details of the necklace region are revealed better in Fig. 2b, which is an electron replica micrograph. The grain boundaries of the small grains are seen to be decorated with overaged γ' which are slightly larger than those inside the warm-worked grains on the adjacent sides. The finest γ' (size 45 nm) is best revealed in TEM of thin foils. Fig. 2c shows a warm-worked grain along with the residual dislocation substructure, which was introduced during the finish forging, and the intermediate sized γ', which serves to stabilize the substructure. The finest γ' appears as small spots in the background.

The fine recrystallized grains of the necklace do not contain any substructure. Strewn mostly in the necklace regions, however, are the MC carbides (average size 15 μm) which are high in Ti, Nb and W and low in Cr and Ni. These carbides are often seen to have readily recognizable shapes (mostly triangular or rectangular as observed in the replicas or opticals).

4.2. Temperature dependence of cyclic life

Fig. 3 gives the variation of the cyclic life with temperature. The curve is based on a least-squares fit and indicates a gradual reduction of fatigue life with increase in temperature up to 922 K and a more drastic decrease beyond 922 K. It is important to note that there is considerable scatter among the specimens tested at room temperature (295 K), 700 K and 922 K.

4.3. Microscopic study of fatigue cracking at room temperature

The main difference between two of the specimens on which progressive microcracking was studied at room temperature by successive replication and which failed at 57 038 and 116 820 cycles respectively were as follows. The initiation time, i.e. the cycle at which the first microcrack was visible at a magnification of × 250 was about three-fold higher in the specimen that had the longer life. Also, microcracking in the specimen with the shorter life was associated with either cracking of an MC-carbide or its decohesion. The crack initiation in the specimen with the longer life appeared to be due to only slip band cracking and was not in any way associated with MC-carbide cracking.

Fig. 4 is a composite picture of the optical micrographs taken from replicas of the shorter-life specimen, that shows the progressive development of two microcracks (nos. 1 and 2) from 30 000 cycles to 48 000 cycles and which finally caused the fracture of the specimen at

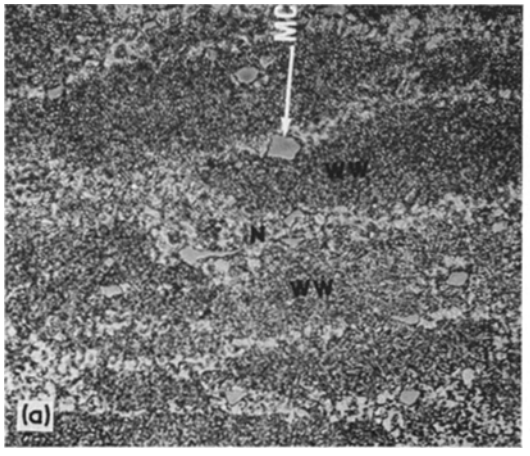

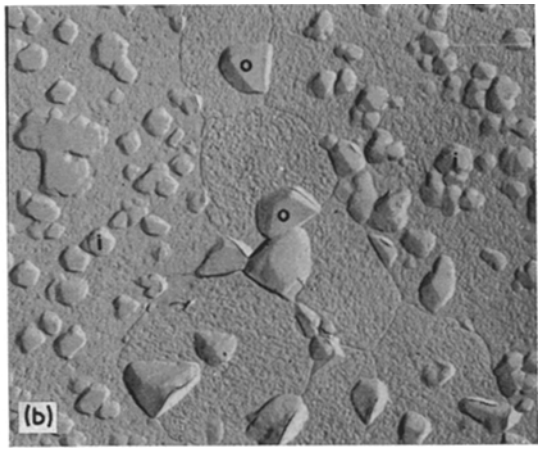

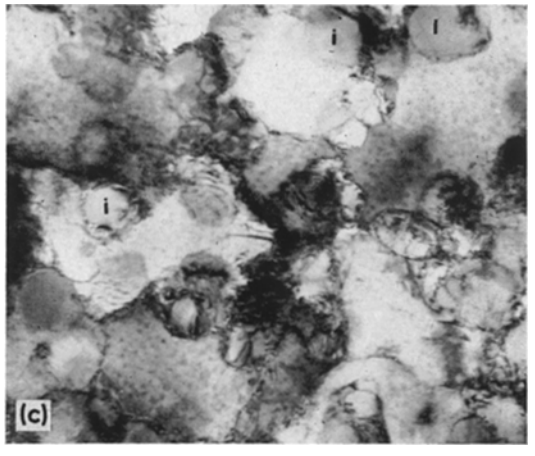

Figure 2 (a) Optical micrograph of necklace René 95 showing warm-worked grains (ww) and the recrystallized necklace region (N), × 400. (b) Electron replica micrograph of necklace showing overaged γ'(0) on the grain boundaries and the intermediate-sized γ'(i) inside the warm-worked grains, × 6400. (c) TEM of a warm worked grain showing the dislocation substructure around the intermediate sized γ'(i), × 16 000.

57 038 cycles. These two cracks were found at the minimum section of the specimen. At 30 000 cycles, in addition to the above, there were two more microcracks present. One was a twin boundary crack approximately 250 μm away from the minimum section but directly above those shown in Fig. 4. This crack (no. 3) propagated only to a very limited extent and did not link up with the main crack at fracture. The other crack (no. 4) was situated approximately 750 μm away from the minimum section and 4000 μm around the specimen (measured on the circumference). This crack propagated until its fatigue area became approximately 25% of that produced by cracks nos. 1 and 2, at which point the specimen broke.

Crack 1 is the bigger of the two and consists of straight segments which change direction as it crosses necklace regions (in other words, grain boundaries) or as it travels across a single warm-worked grain itself. There is a small MC carbide, MC-1, that has been fractured, which is difficult to see at × 250 but is clearly seen in Fig. 5 at × 800. Crack 2 seems to have originated by the decohesion of an MC carbide, MC-2, from the matrix. There is no visible propagation of these cracks until 45 000 cycles. At 44 000 cycles, slip activity was observed at the site marked S, which eventually became a microcrack. Significant linkage of the microcracks occurred between 44 000 and 46 000 cycles and continued until 48 000 cycles. The propagation of this crack was ultimately responsible for the failure of the specimen.

Similar events were observed near crack 4, which seems to be associated with decohesion of an MC carbide, MC-4, from the matrix (Fig. 6). A comparison of Figs. 3 and 6 shows that the area covered by the fourth crack at 46 000 cycles is much less than that covered by the single crack formed by the linkage of cracks 1 and 2. Although there were other MC carbides in the neighbourhood of cracks 1 and 2, they were found to be intact and not cracked during the life of the specimen.

A complete examination of the fracture surface in the scanning electron microscope showed that the fatigued area of cracks 1, 2 and 4 near the surface of the specimen consisted of straight planar facets, typical of stage I, crystallographic

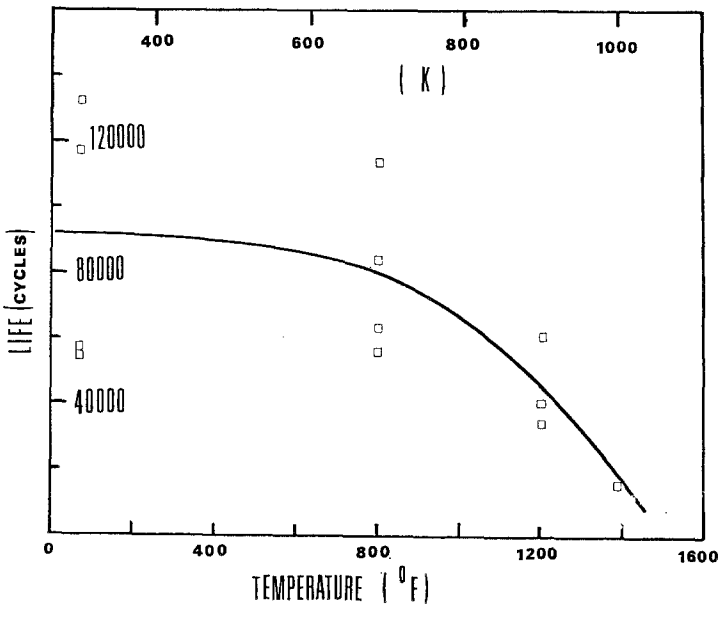

Figure 3 Variation of cyclic life with temperature.

fracture. Fig. 7 shows a typical stage I area, which was always followed by a stage II area containing striations (Fig. 8). Both these areas can be seen in Fig. 9, which is a SEM micrograph of the regions near cracks 1 and 2, as viewed from the edge of the fracture surface at an angle. A comparison of Figs. 9 and 3 indicates that the cracks propagated in stage I mode until about 46 000 cycles, at which the fatigued area reveals indications of transition to stage II mode and further propagation in that mode until failure.

Generally, it was very difficult to locate the remnants of cracked carbides in stage I area. However, many carbides were seen in the stage II area, all of them in the fractured condition (Fig. 10). On the surface of the specimen, many had cracked across their short dimensions or separated from the matrix by decohesion at the carbide-matrix interface. Fig. 11 is a replica electron micrograph of a cracked MC carbide in the necklace region. The cracks did not seem to follow grain boundaries, in general. However, whenever twin boundaries were present in the way, the cracking followed the twin boundary. Although slip markings were not conspicuous at the stresses employed in the investigation, indications were obtained where the straight segments of the cracks appeared parallel to faint traces of slip lines produced during cycling. Fig. 12 is an example of this.

In order to find out if the initial microcrack generation and propagation have any relation to slip bands, one specimen was fatigued at 1482 MN m^{-2} maximum with the same R value. Examination of surface replicas did show a strong correlation between the slip extrusion markings and the initial development of the microcracks. In most of the cases, the cracks started out from a carbide and followed the slip lines (Fig. 13a). In a few instances isolated slip lines were found to develop into microcracks (Fig. 13b). The fatigue fracture at this stress level showed similar features to that found in specimens tested at 1275.5 MN m^{-2}. It can, therefore, be concluded that the stage I cracking at 1275.5 MN m^{-2} also develops parallel to well-defined slip bands.

Transmission electron microscopic study showed a general increase in dislocation density with cycling. Fig. 14 shows a warm-worked grain in the specimen cycled to 8000 cycles, in which the dislocations form braids from the activity in the existing structure. The increase in dislocation density as a result of fatigue cycling was found to be quite uniform over the length of the sub-size specimen tested to 8000 cycles. Foils close to the fracture surface near the fatigued area taken from the standard LCF specimen showed a much larger accumulation of dislocations which was again homogeneous with no banding of deformation occurring. This is again

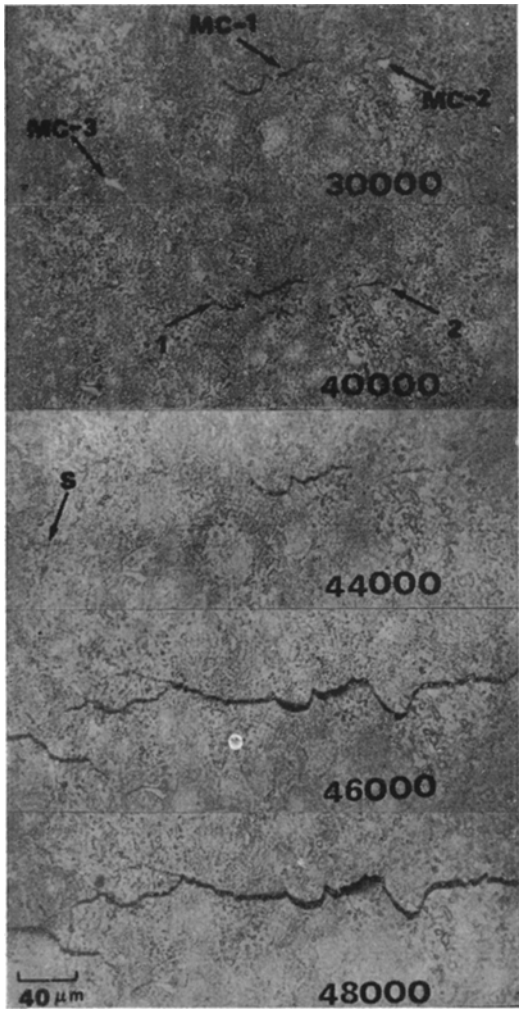

Figure 4 Optical micrograph showing the development of microcracking from 30 000 to 48 000 cycles. MC-1, MC-2, MC-3 are MC carbides.

representative of a large number of foils examined. The deformation in the fine recrystallized grains was also very homogeneous in that the inter slip band spacing was extremely small (Fig. 15).

An extensive replica study of the development of fatigue cracking in the specimen cycled under the same conditions of 1275.5 MN m^{-2} and an R value of 0.05 at room temperature and which broke at 116 820 cycles revealed only one initiation point at the surface. Fig. 16 shows the SEM picture of the initiation area which is a warm-worked grain. The initiation was characterized by cracking along what appeared to be slip planes (note the arrow), although the grain

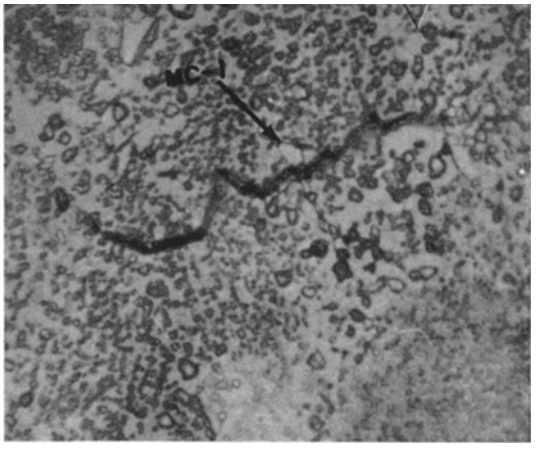

Figure 5 Magnified picture of cracking near MC-1, × 800.

did not show any evidence of slip band formation except that which ultimately became the crack itself. The crack initiation was not associated with any MC carbide cracking. The crack was first seen at 90 000 cycles and propagated in stage I mode until 108 000 cycles.

4.4. Fatigue at elevated temperatures

The replica technique was not successful in revealing the phenomenon of microcracking on the surface of the specimen tested at 700 K because of slight oxidation and occasional subsurface initiation and propagation. At 922 K, the crack initiation and propagation was always subsurface; hence the replica technique could not be employed at all. However, the SEM

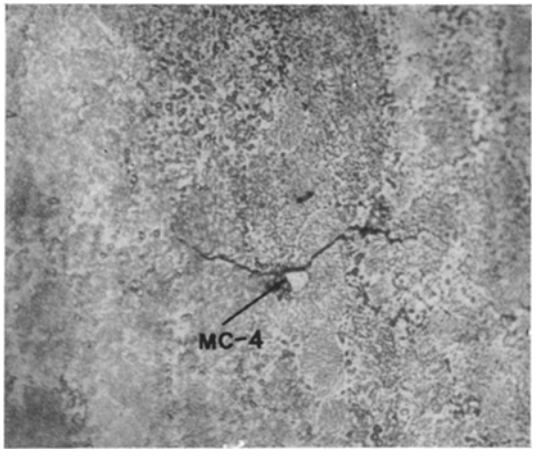

Figure 6 Cracking near MC-4 by decohesion at the carbide matrix interface, × 250.

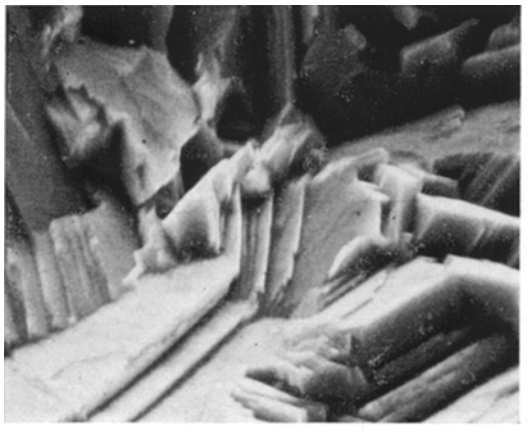

Figure 7 SEM of stage I fracture surface, × 2100.

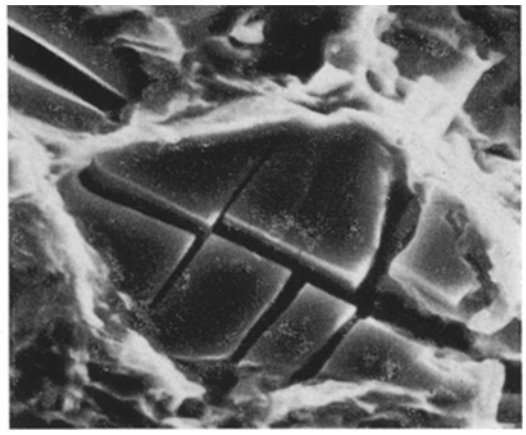

Figure 10 Cracked MC carbides in stage II area, × 2100.

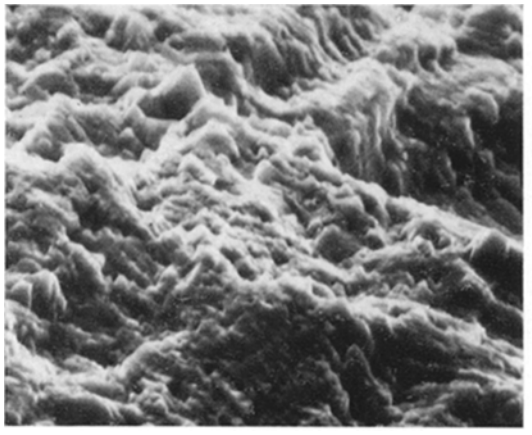

Figure 8 SEM of stage II area, × 2100.

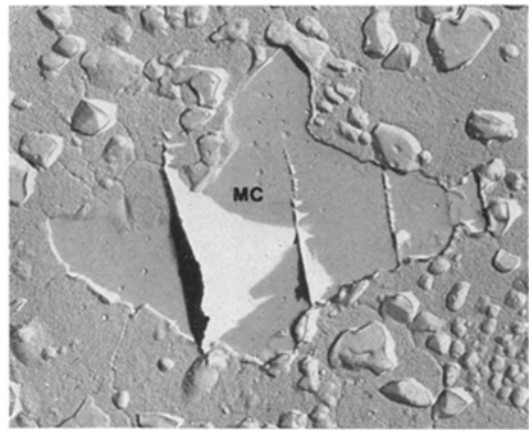

Figure 11 Replica micrograph of a cracked MC carbide in the necklace region, × 2500.

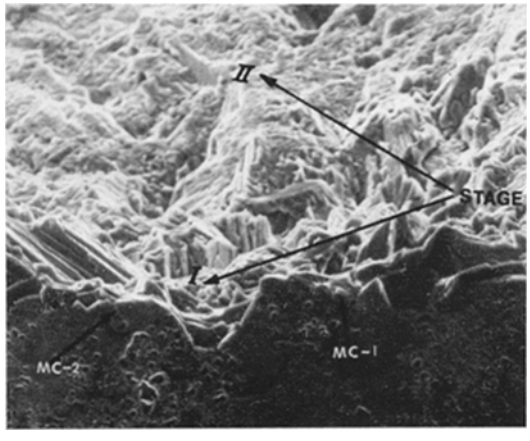

Figure 9 SEM of the stage I and II area on the fracture surface. Note the MC-2 remaining intact on the surface of the specimen, × 420.

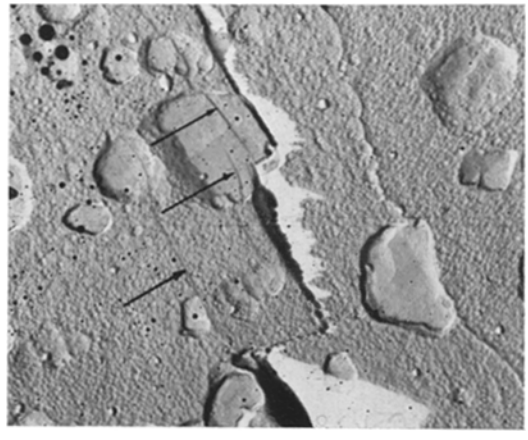

Figure 12 Replica micrograph showing the path of the crack parallel to faint traces of slip lines (arrow), × 8500.

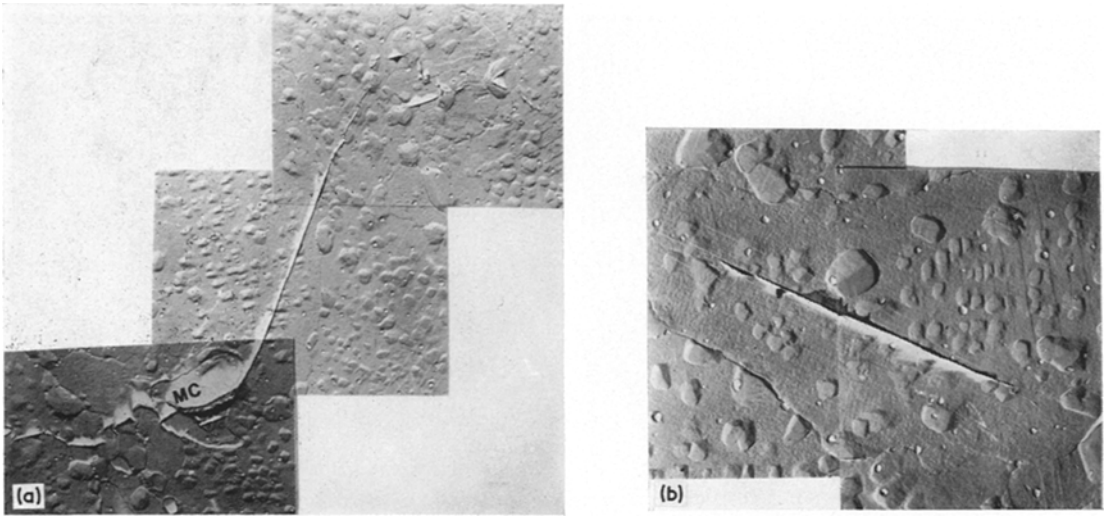

Figure 13 (a) Replica micrograph of cracking originating from a cracked carbide. The propagation seems to be along planes parallel to the slip lines, × 3150. (b) Replica micrograph of microcracking along a slip extrusion in the absence of any cracked brittle constituents, × 3250.

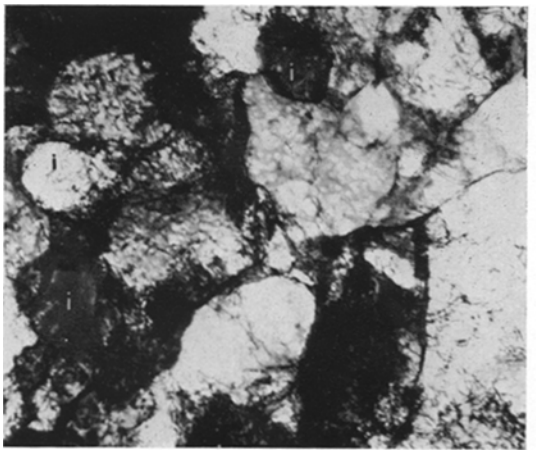

Figure 14 Warm-worked grain cycled 8000 times, × 18 500.

Figure 15 Slip band formation in a necklace grain, × 15 500.

examination of the fracture surfaces showed that the mode of fracture was similar to that observed at room temperature in that the fatigued area consisted of stage I and stage II. Although there was no direct evidence of MC cracking near stage I regions in specimens tested at 700 K and which had shorter lives, the initiation region in subsurface cases showed unusual stage I areas as shown in Fig. 17. It must be mentioned that such cracks (arrows) as shown in Fig. 17 were not observed near stage I areas of specimens that had longer lives. At 922 K, definite evidence of the presence of MC carbide that had undergone partial decohesion from the fracture surface was seen near the stage I area. Fig. 18 shows such an area in the specimen which failed at 40 952. The identity of the carbide was also verified using the energy dispersive X-ray method.

5. Discussion

5.1. Deformation behaviour in fatigue

The conventional superalloys have been known to deform at room temperature, and at temperatures up to approximately 1033 K in coarse,

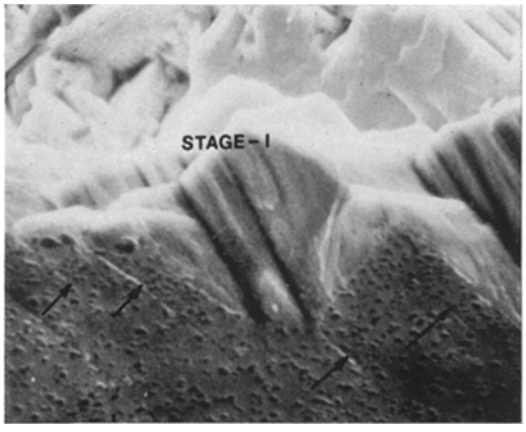

Figure 16 SEM of the initiation site of stage I cracking in a specimen that failed at 116 820 cycles. The initiation occurred in a warm worked grain along straight segments. Note the crack that has branched off at an angle from the fracture surface (arrow), × 1680.

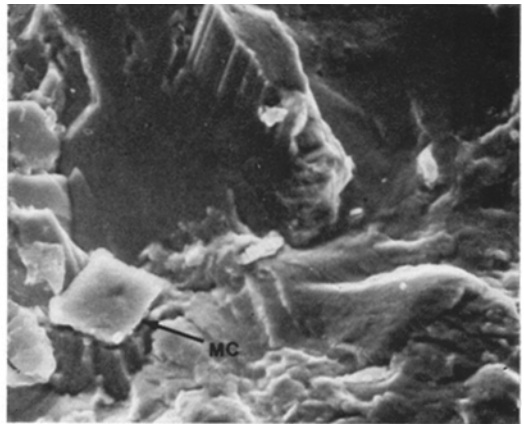

Figure 18 Sub-surface stage I initiation at 922 K. Note the MC carbide (arrow) that has undergone partial decohesion from the matrix, × 850.

planar mode [2]. In a recent study on the tensile behaviour of René 95 at temperatures up to 1033 K [7], it was observed that the slip bands that were formed in necklace René 95 during deformation were not as intense or coarse as those found in Mar-M 200 or other superalloys reported in earlier works. On the other hand, deformation seemed to be quite homogeneously distributed both in the necklace and in the recrystallized grains. Observations of deformation substructures found in samples deformed in fatigue also point to a very homogeneous mode of deformation occurring near the fracture initiation sites prior to cracking and possibly also near the crack tips and areas adjacent to the fracture path. As in the tensile study, it may be concluded that the dislocation substructure retained in the warm-worked grains as a result of TMP was very effective in dispersing slip, which in turn prevented early formation of intense slip bands and forced the deformation to take place more homogeneously throughout the material. The very fine necklace grains which have an approximate size of 4 μm are believed to act in the same manner, as it is well known that very small grain sizes are effective in dispersing slip leading to more homogeneous deformation. It may be worthwhile to note that the inter-slipband spacing in the recrystallized grains are very fine (less than 0.5 μm, see Fig. 16).

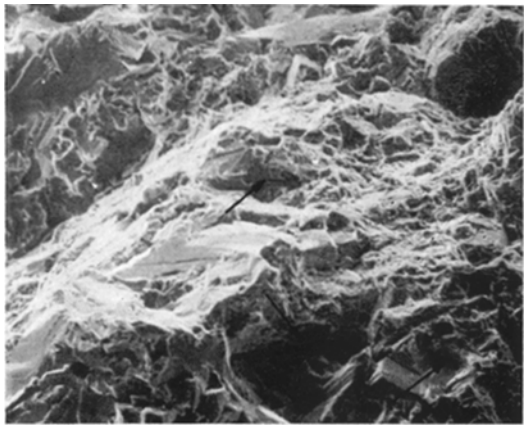

Figure 17 Sub-surface stage I initiation at 700 K. Note the unusual mode of cracking (arrow), × 215.

The lack of intensity or sometimes even the absence of slip extrusions in the case of deformation (tensile monotonic, and fatigue) of René 95 stands in contrast to those found in superalloys such as Mar-M 200 [8] or Inconel 718 [9]. In the present study, slip lines were absent in specimens cycled at 1275.5 MN m^{-2}. However, when the stress was increased to 1482 MN m^{-2} they could readily be seen. Still, the extrusion height (slip band height) was not as large as expected when a microcrack appeared. This behaviour is similar to that observed in the tensile study, where there was no apparent increase in the slip band height as René 95 was deformed to higher and higher levels of strain. It is believed that this is due to the defect substructure present in the warm-worked grains. The residual substructure is believed to be very effective in dispersing slip and thus

forcing the materials to deform more homogeneously.

After extensive deformation, it is possible, however, that well defined slip bands could eventually form and become more and more intense with continued cycling as a result of dislocation accumulation. Cracking would then eventually occur on these bands leading to the extensive stage I facets observed in René 95. Absence of any dimples in the stage I area also indicates that the cracking followed such a planar mode through the recrystallized (necklace) grains. These planar bands of deformation can intersect within a grain itself or such bands from adjacent grains can intersect at the grain boundary leading to a situation in which the crack changes direction as it propagates. The facets shown in Fig. 7 are believed to have originated in the above manner.

5.2. MC cracking

Fig. 11 reveals the mode of cracking of an MC carbide, which is in the necklace region and surrounded by about six small grains. The traces of the cracks suggest also one prominent plane for fracture of these carbides (see also Fig. 10). It ought to be realized that the replicas reveal only the size of a carbide in two dimensions. It may be that, for example, the MC carbide associated with crack 1, although small as seen from the surface, could have been large in the third dimension (i.e. into the specimen). In the scanning electron microscope, only a few small broken pieces of the MC-1 carbide could be identified. In general, it was very difficult to locate the remnants of MC carbides in the stage I area as the remnants were very small in size (due to breakage and subsequent removal from their location). In the stage II area, and in the overload region, most of the carbides remained in their original locations, although broken.

There was always some MC carbides that did not crack at all during the fatigue cycling although these were found in the minimum section. Also, there was no correlation between the size of the carbides as viewed from the surface (i.e. in the replica) and their ease of fracturing. In the tensile study, it was found that a strain of 0.01 had to be reached before all the MC carbides cracked. The stress employed in this study, 1275.5 MN m^{-2}, is just near the 0.2% yield strength value. Therefore, not all the grains would have had the chance to undergo sufficient deformation to cause all the carbides to fracture.

Observation of replicas suggests that the fracture of MC carbides probably accelerates or aids the initiation of fatigue cracks. The characteristics of fracture of these carbides reported earlier suggest that the cracking is deformation induced. Evidence obtained in the tensile study also points to the above conclusion.

The absence of any cracked MC carbides at the site of the initiation in the case of the specimen which had longer life (Fig. 17) may suggest that the carbides are responsible for earlier initiation of stage I cracks in the specimens that had lower lives. Comparing the lives of the two specimens which failed at 57 038 and 116 820 cycles, respectively, the total life of a fatigue crack from its initiation to final fracture is approximately the same, 27 038 and 26 820 cycles ($\pm$ 5000 cycles) respectively. Also the time spent in stage I mode is also the same, 16 000 and 18 000 cycles ($\pm$ 5000 cycles) respectively. On the other hand, the crack initiation was noticed at 30 000 and 90 000 cycles ($\pm$ 5000) cycles respectively. From this limited data, one may conclude that the scatter in the time of propagation of a crack is far less than that in its initiation.

6. Conclusion

The present study points out that René 95 retains very high resistance to low cycle fatigue cracking even up to 922 K as evidenced by the data in Fig. 3. It is believed that such improved properties in low cycle fatigue are due to the homogeneous deformation characteristics of necklace René 95. The dislocation substructure in the warm-worked grains seem to be very effective in dispersing slip throughout a grain, thus forcing the material to deform homogeneously. A similar effect is also provided by the presence of necklace grains, whose size is extremely small (4 μm).

The study also shows that the number of load cycles to produce crack initiation can be strongly affected by brittle constituents of the microstructure. In the present investigation, replication of cracking phenomenon in the case of the specimen which lies higher in the scatter band of Fig. 3 showed absence of any MC carbide cracking associated with the initiation site. However, in the case of the specimen near the lower side of the scatter band, cracking of MC carbide seemed to play a significant role. It is logical, therefore, to assume that removal of the carbides or reduction in their size might narrow the scatter

and move the data to the upper side of the band. Again, concluding from the limited data available, this would happen because of the enhancement of the initiation time for stage I cracking.

Acknowledgement

One of the authors wishes to acknowledge the support of National Research Council during his tenure as a Research Associate at the Air Force Materials Laboratory.

References

1. C. H. WELLS and C. P. SULLIVAN, *ASM Trans. Quart.* **57** (1964) 841.
2. M. GELL and G. R. LEVERANT, *Trans. Met. Soc. AIME* **202** (1968) 1869.
3. C. H. WELLS and C. P. SULLIVAN, *ASM Trans. Quart.* **60** (1967) 217.
4. G. R. LEVERANT and M. GELL, *Trans. Met. Soc. AIME* **245** (1969) 1167.
5. G.P.SABOL,T.F.HENGSTENBERG and D. M. MOON, "Electron Microscopy and Structure of Metals", edited by G. Thomas (University of California Press, Berkeley, 1972) pp. 753-63.
6. M. N. MENON, Air Force Materials Lab. Technical Report, AFML-TR-73-180 (1973).
7. M. N. MENON and W. H. REIMANN, *ibid*, AFML-TR-74-100 (1974).
8. M. GELL, G. R. LEVERANT and C. H. WELLS, ASTM-STP-467 (1970) 113.
9. M. F. HENRY, G.E. Report No. 72CRD 100, March 1972 (available from Technical Information Exchange, P.O. Box 43, Building 5, Schenectady, NY 12301).

Received 31 December 1974 and accepted 12 February 1975.